

NJC

Accepted Manuscript



This is an *Accepted Manuscript*, which has been through the Royal Society of Chemistry peer review process and has been accepted for publication.

Accepted Manuscripts are published online shortly after acceptance, before technical editing, formatting and proof reading. Using this free service, authors can make their results available to the community, in citable form, before we publish the edited article. We will replace this *Accepted Manuscript* with the edited and formatted *Advance Article* as soon as it is available.

You can find more information about *Accepted Manuscripts* in the [Information for Authors](#).

Please note that technical editing may introduce minor changes to the text and/or graphics, which may alter content. The journal's standard [Terms & Conditions](#) and the [Ethical guidelines](#) still apply. In no event shall the Royal Society of Chemistry be held responsible for any errors or omissions in this *Accepted Manuscript* or any consequences arising from the use of any information it contains.



Journal Name

ARTICLE

Highly selective colorimetric and reversible fluorometric turn-off sensors based on pyrimidine derivative: mimicking logic gate operation and potential application

Received 00th January 20xx,
Accepted 00th January 20xx

DOI: 10.1039/x0xx00000x

www.rsc.org/

Neha Gupta, Divya Singhal, Ashok Kumar Singh*
Department of Chemistry, Indian Institute of Technology-Roorkee,
Roorkee-247667, India

*E-mail: akscyfcy@iitr.ernet.in

Abstract

Two novel pyrimidine based 5-(2-hydroxybenzylideneamino)-6-amino-2-mercaptopyrimidin-4-ol (S_1) and 5-(3-nitrobenzylideneamino)-6-amino-2-mercaptopyrimidin-4-ol (S_2) receptors have been synthesized and characterized by various techniques. Both receptors showed 2:1 complexation stoichiometry with Ni(II) having binding constant 2.9×10^6 (S_1) and 2.1×10^6 (S_2) calculated by Job's plot based on the UV-Vis absorption studies. The binding stoichiometry was also supported by ESI mass spectra and NMR titration. The addition of Ni(II) to both chemosensors, S_1 and S_2 leads to the fluorescence quenching of S-Ni(II), forming an off sensing type system with the limit of detection 33 μM and 48 μM respectively. It was observed that S_1 and S_2 achieved electrochemical changes in reduction and oxidation potentials after the addition of nickel metal ion. DFT calculations have revealed that the energy gap between HOMO and LUMO of S_1 , S_2 are significantly decreased upon coordination with Ni(II) in gas phase.

Introduction

In recent years a great deal of research has been

attracted towards transition metal ion detection due to their environmental and biological importance. Nickel is an essential trace element for supporting life, such as respiration, metabolism and biosynthesis¹. Nickel compounds have many industrial and commercial uses, and the progress of

^a Address here.

^b Address here.

^c Address here.

† Footnotes relating to the title and/or authors should appear here.

Electronic Supplementary Information (ESI) available: [details of any supplementary information available should be included here]. See

DOI: 10.1039/x0xx00000x

industrialization has led to increased emission of pollutants into ecosystems². It has been used in industrial applications such as stainless steel, jewellery, electroplating, Ni-Cd batteries, machinery, tools and as a precursor for catalyst³. However a higher uptake of nickel can cause a variety of pathological effects on the human body as in a form of lung cancer, prostate cancer, larynx cancer, lung embolism, asthma and chronic bronchitis, pneumonitis and dermatitis⁴. In the various literature, several review studies have been reported on the recognition fluorogenic unit which is responsible for the selectivity and binding efficiency of the chemosensor. Several N-heterocycles such as, triazole, thiazole, pyridine, pyrrole, quinoline, or imidazole and their derivatives are utilized as recognition units. Such as pyrimidine derivatives are appropriate objects for using as excellent sensing materials and also have a variety of biological and medicinal applications. The efficiency of pyrimidine derivatives to form both coordination and hydrogen bond make them assuring to the use as sensing probes. The simplicity and cost-effectiveness are always a matter of concern for optical chemosensor. Thus, here we report the facile and inexpensive synthesis of two novel pyrimidine based colorimetric and fluorogenic receptors which has been obtained in pure powdered form without any column chromatographic purification.

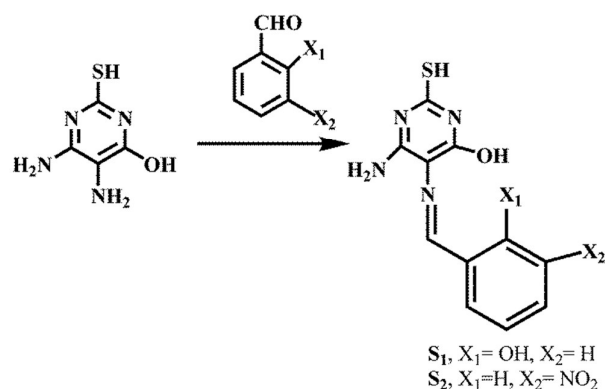
In order to quantify nickel ions, several analytical techniques of high cost such as inductively coupled plasma optical emission spectrometry⁵, coated wire ion selective electrode⁶,

microwave induced plasma⁷, electrothermal atomic absorption spectrometry⁸, and spectrophotometry⁹ have been used. Many of these pretreatment techniques are, however complicated, time consuming and not suitable for quick response. In recent time the most oftenally utilize method is an optical sensing, because of low cost and simple handling. There are several mechanisms which support the fluorescence behavior for cations and anions as internal charge transfer (ICT), chelation enhanced fluorescence (CHEF), photoinduced electron transfer (PET) and deprotonation mechanisms.

To design efficient colorimetric sensor with open coordination sites which has high selectivity and sensitivity for Ni(II) ion, two receptors have been synthesized by condensation method. A significant color change of receptors solution was occurred after addition of Ni(II) ion as light yellow to dark yellow with red shift. These two receptors S₁ and S₂ have shown fluorescence quenching after the recognition with Ni(II) ion, it caused by the paramagnetic nature of Ni(II) ion. Further, we have been investigating the electrochemical behavior of the two receptors by cyclic voltammetry experiment. In the recognition, 2:1 stoichiometry was corroborate by the Jobs plot as well as theoretical aspects. The reversible behavior of chemical receptors is presented with the logic gate application.

Results and discussion

Two Schiff bases were synthesized in good yield by employing a simple synthetic route of condensation in dry methanol. 4,5-Diamino-6-hydroxy-2-mercaptopyrimidine was used as common amine with a different aldehyde (scheme 1).



Scheme 1. Synthesis of receptors S_1 and S_2 .

In order to investigate the recognition ability of both receptors with different metal ions, the preliminary studies have been executed. UV-Vis studies demonstrated the affinity of S_1, S_2 towards Ni(II) ion over various metal ions, and upon the addition of nickel acetate, a sudden color change from light yellow to dark yellow was observed. (ESI Fig. 1). Thus we have conducted colorimetric

studies by using equimolar solutions (1.0×10^{-4} M) of S_1, S_2 and metal ions in DMF. The sudden color change of the receptors was most probably due to the recognition or deprotonation of $-\text{OH}$ groups upon addition of Ni(II) ion¹⁰.

UV-Vis Analysis

S_1 and S_2 displays a more intense color change in the presence of Ni(II) on the behalf of strong metal-receptor interaction, whereas no significant changes were observed with Mg(II), Ca(II), Pb(II), Hg(II), Fe(II), Sr(II), Mn(II), Cu(II), Mo(II), Ag(I), Co(II), Zn(II) and Cd(II) ion. Upon the addition of Ni(II), the UV-Vis Spectra of S_1, S_2 was showing red-shift that indicates a charge transfer interaction between the receptor moiety and nickel metal ion (Fig.1). Binding stability was examined by monitoring over the time, the colorimetric changes were observed to measure the strength of interaction between the receptor and metal ion¹¹. Usually, it has been observed that chemosensors have long response time, but in case of these receptors the binding process with Ni(II) ion is found to very fast i.e. less than 13 sec and remained quite stable.

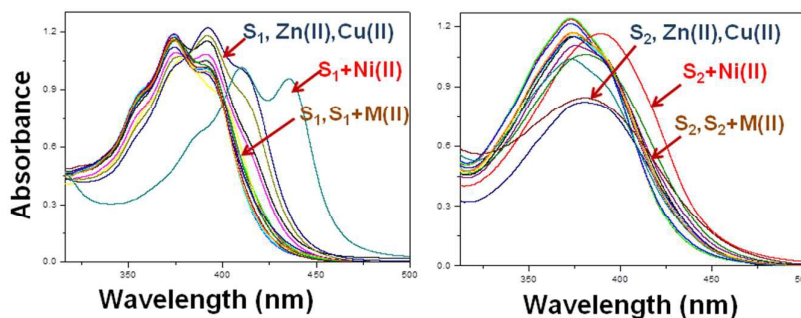


Fig. 1 UV-Vis studies of S_1 and S_2 (4×10^{-5} M) with all metal ions.

Journal Name

ARTICLE

It can be observed that the colorimetric property of the S-Ni(II) is also stable with time (ESI Fig. 2).

Stoichiometry and binding sites

To ensure the binding sites of the both receptors response, the binding stoichiometry of S_1 and S_2 was calculated from Job's plot on the basis of UV-Vis absorption studies¹². Equimolar solutions (4×10^{-5} M) of receptors S_1 , S_2 and Nickel metal ion were prepared in DMF. To determine the binding stoichiometry of S+Ni(II), we carried out absorption titration experiments in the presence of varying mole-fractions of Ni(II) in DMF. The stoichiometry was established by Job's plot between the mole fraction and absorption maximum changes at 435 nm for S_1 and 409 nm for S_2 (Fig.2). Upon the addition of 0-6 mL of Ni(II) (with the equal span of 0.5 mL), the absorption maxima of S_1 and S_2 were quenched at 392 nm (S_1) and 374 nm (S_2) and a new band appeared at 435 and 409 nm respectively. Maximum absorbance was obtained at mole fraction 0.66, indicating the stoichiometry of S + Ni(II) was 2:1. S_1 obtained more binding ability in comparison to S_2 , the binding constant calculated by Job's plot were 2.9×10^6 for S_1 and 2.1×10^6 for S_2 .

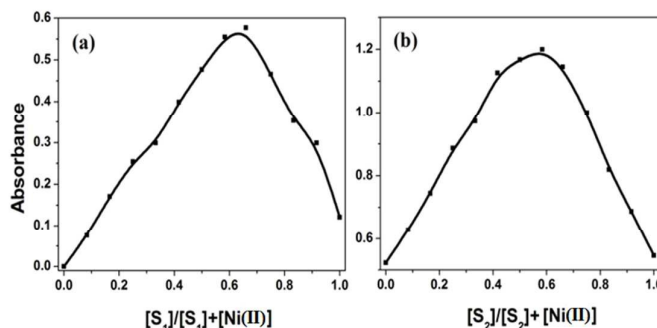


Fig. 2 Job's plot of equimolar concentration (4.0×10^{-5} M) of receptors S_1 (a) and S_2 (b) with Ni (II) ion.

The stability constants were calculated by the following expression¹³:



$$K_f = \frac{[AS]}{[A][S]} \quad (2)$$

$$K_f = \frac{[A_2/A_1]}{[1 - A_2/A_1][C_S - C_M \times A_2/A_1]} \quad (3)$$

Where, C_S is the receptor concentration, C_M is the metal concentration, A_2 is the actual absorbance, A_1 is the absorbance at break point.

The Job's curve for both receptors exhibited in Figure 2. The isosbestic points at 402 nm (S_1) and 312 nm, 381 nm (S_2) clearly indicates that there was a new complex formation with certain stoichiometry ratio between host and guest via internal charge transfer¹⁴ (Fig. 3a, 3b).

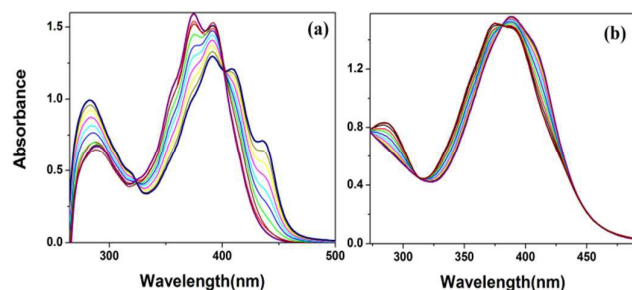


Fig.3 UV–Vis titration spectra (a and b) of receptor S_1 , S_2 (5×10^{-5} M) upon addition Ni(II) ion in DMF solvent. (0, 0.3, 0.6, 0.9, 1.2, 1.5, 1.8, 2.1, 2.4, 2.7, 3) equivalents of Ni(II) ion.

Similar to Job's plot, the binding stoichiometry was further supported by ESI mass spectrum and ^1H NMR titration along with binding site confirmation as shown in (Fig 4). The ESI mass spectrum of a mixture of receptors and $\text{Ni}(\text{CH}_3\text{COO})_2 \cdot 4\text{H}_2\text{O}$ revealed the formation of S-Ni(II) complex through coordination bond, which showed a sharp peak at $m/z_{\text{calcd}} = 581.92$ calculated, found 581.25 for $[2S_1\text{-Ni(II)+H}]$ and $m/z_{\text{calcd}} = 639.50$ calculated, found 639.24 for $[2S_2\text{-Ni(II)+H}]$ (ESI Fig.3). From NMR study, we have investigated the interactions between the receptors and nickel ion with the addition of different equivalent of nickel ion (0, 0.3, 0.5, 0.8) to receptors S_1 , S_2 in DMSO-d_6 . Upon the addition of 0.5 equiv., the hydroxyl group of amine moiety is completely disappeared along with the downfield shift of imine proton from 9.75 ppm to 9.83 ppm (S_1) and 9.76 ppm to 9.92 ppm (S_2) through diamagnetic deshielding indicating that there is a

new complex formation (2:1) between the $-\text{OH}$ group, imine $\text{CH}=\text{N}$ moiety of pyrimidine and nickel ion. There was no significant change on SH proton and the rest of the aromatic region protons. It was observed that further addition (more than 0.5 equiv.) of nickel ion did not change ^1H NMR spectra¹⁵ (ESI Fig. 4). The both S-Ni(II) complex optimized as square planar geometry in gas phase, which shows the diamagnetic nature of nickel metal ion, cause of deshielding of protons. The NMR titration evaluated that Ni(II) is coordinating through nitrogen and oxygen atom of pyrimidine moiety in S-Ni(II) complex.

Fluorescence studies

Similar to the absorption study of these two receptors, we have also investigated the photophysical properties of receptors in DMF. To scrutinize the practical ability of both S_1 and S_2 , the competitive binding studies with other metal ions have been introduced (Fig. 5 and 6). It has been observed that other metal ions show minimum disruption in fluorescence spectra of both compounds. Fluorescence emission of S_1 and S_2 (5×10^{-6} M) did not show any appreciable interference after the addition of different metal ion. S_1 showed the maximum excitation at 392 nm and emission at 520 nm while S_2 showed the maximum excitation at 374 nm and emission at 441 nm which shows a large stoke shift.

Journal Name

ARTICLE

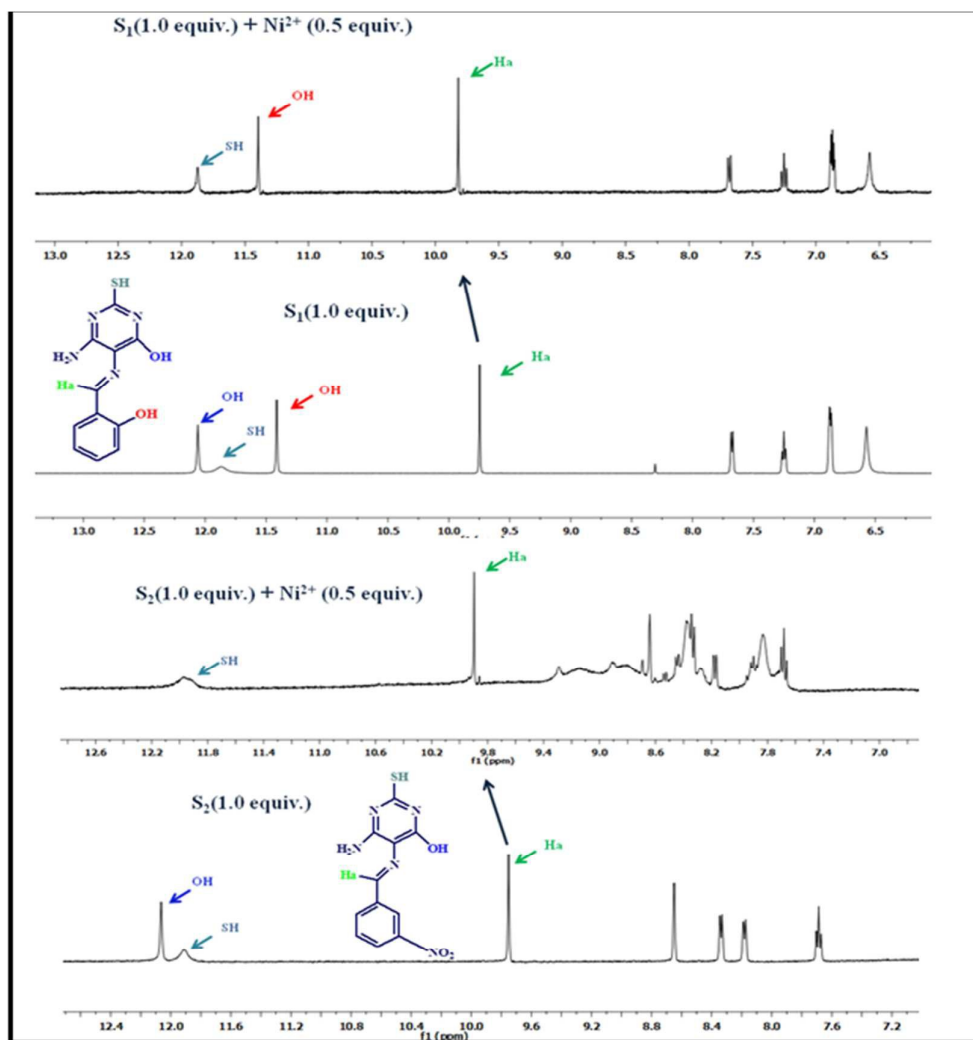


Fig.4 ^1H NMR titration of S_1 and S_2 with $\text{Ni}(\text{II})$ ion.

After the gradual addition of nickel ion concentration, fluorescence quenching phenomenon is occurred¹⁶ (Fig. 7 and 8). The electron or energy transfer could be a possible mechanism for remarkable quenching with $\text{Ni}(\text{II})$

ion. The Stern-Volmer plot clearly indicates that the static nature of quenching. The energy transfer mechanism provides a pathway for the contribution to the nonradiative deactivation of the excited state to a significant extent¹⁷.

Journal Name

ARTICLE

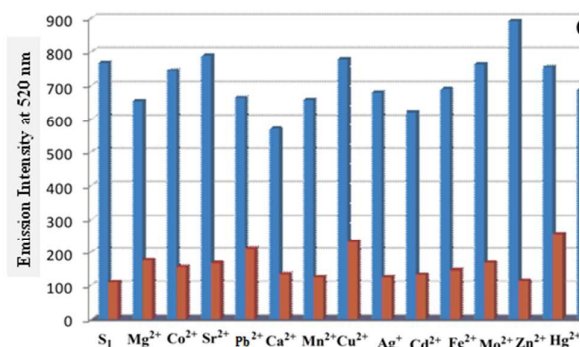


Fig.5 Interference study with different metal ion at 520 nm, S_1 + metal ions (blue bar) and S_1 + metal ions + Ni(II) (red bar)

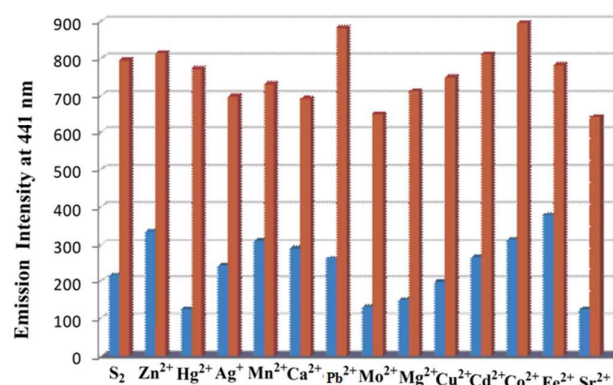


Fig.6 Interference study with different metal ion at 441 nm. S_2 + metal ions (red bar) and S_2 + metal ions + Ni(II) (blue bar).

For the calculation of limit of detection, fluorescence intensity of S_1 and S_2 at each concentration of Ni(II) added, normalized between the maximum fluorescence intensity, found at zero equiv. of Ni(II), and the minimum fluorescence intensity, found at 5×10^{-6} M of Ni(II). Limit of detection have been calculated by using the

intercept of a plot between $(I - I_{\min}) / (I_{\max} - I_{\min})$ and $\log[\text{Ni(II)}]^{18}$ and found to be 33 and 48 μM for S_1 and S_2 respectively ESI Fig.5.

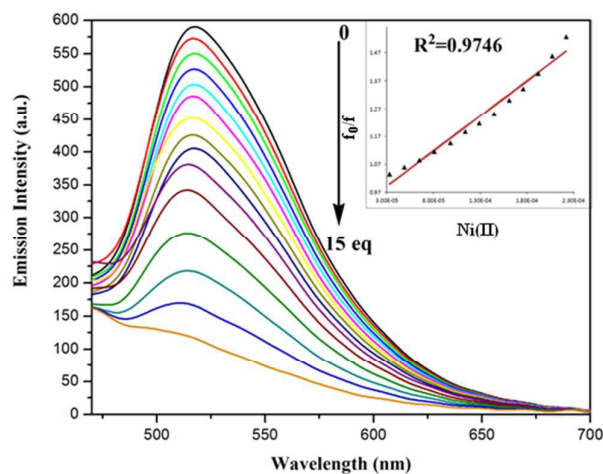


Fig.7 Emission spectra of S_1 (5.0×10^{-6} M) in the presence of varying concentration of Ni(II) at λ_{ex} 392 nm. (inset–change in emission intensity with number of equivalents of Ni(II))

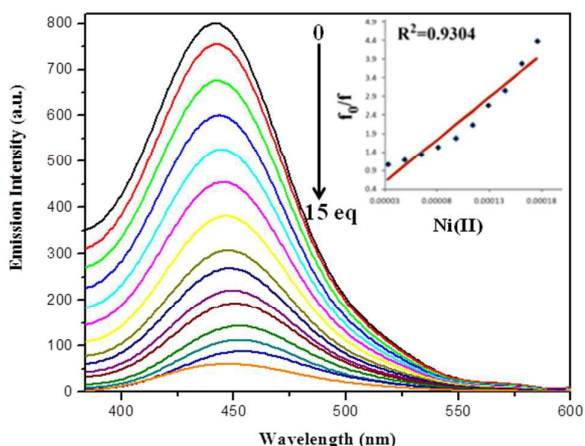


Fig.8 Emission spectra of S_2 (5.0×10^{-6} M) in the presence of varying concentration of Ni(II) at λ_{ex}

374 nm (inset–change in emission intensity with number of equivalents of Ni(II)).

Optimization of analytical conditions

The potential selectivity of both receptors was determined as a function of pH over a wide pH range (1-14). A 25 mL stock solution (4×10^{-5} M) of both receptors was prepared in DMF as the receptors are sparingly soluble in water. The pH was adjusted with the addition of aqueous 0.5 M HCl and 1M NaOH. The optical studies of both S_1 -Ni(II) and S_2 -Ni(II) with respect to different pH affirmed that both receptors predominantly work between pH 5-11 and 6-12 respectively (ESI Fig. 6).

At low pH (1-4) receptors did not show any changes with Ni metal ion in absorption studies. On increase pH 12-14 selectivity of sensors was decreased. The effect of pH on the emission spectra of S_1 and S_2 ($5 \mu\text{M}$) was examined in the absence and presence ($5 \mu\text{M}$) of Ni(II) (Fig. 9). At $\text{pH} < 5$, the fluorescence intensity of both receptors was relatively lower owing to the protonation, as the high $\text{pH} > 12$, OH^- will compete with receptors to bind Ni(II), which influenced the detection of Ni(II). S_1 and S_2 chemosensors work well in wide range of 5–11 and 6–11, respectively for the detection of Ni(II) ion. That proves the utility of both receptors to work as a sensor under physiological pH conditions. The effect of water content on absorption studies as well as fluorescence

intensity of both receptors ($5 \mu\text{M}$) has been studied. It is observed that the selectivity and sensitivity of both receptors have been diminished with increasing the content of water. Receptor S_1 has shown selectivity with nickel ion up to 40% water while S_2 has shown up to 20% water (ESI Fig. 7). The sensitivity of the receptors has gradually decreased after their respective percentage. Thus receptor S_1 has more real-purpose applicability than S_2 .

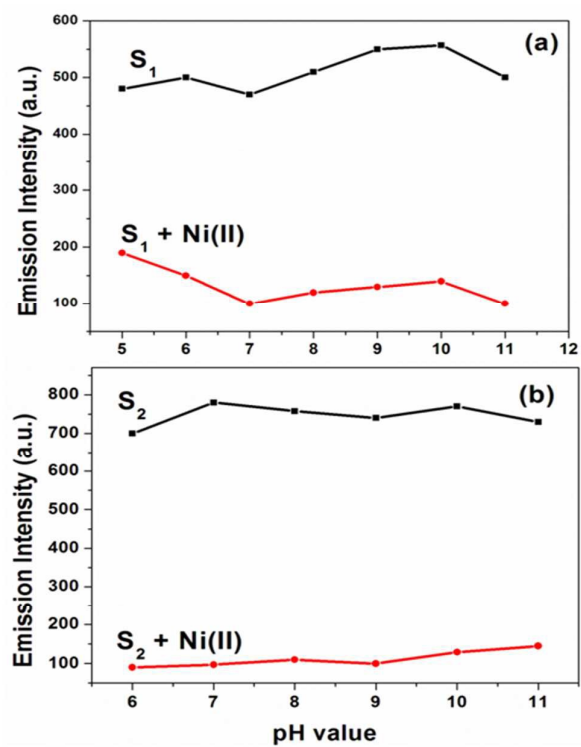


Fig. 9 Effect of pH on emission spectra of S_1 (a) and S_2 (b) in DMF without and with Ni(II).

Electrochemical behavior of sensors

Cyclic Voltammetry Experiment

To investigate the redox properties of both receptors and their complexation with Ni(II), the cyclic voltammograms of receptors S_1 , S_2 and S -Ni(II) were recorded in DMF solution containing 0.1 M TBAP. The cyclic voltammogram of S_1 was displayed two reversible oxidation peak at 0.91 V and 1.33 V and non reversible reduction peak at -0.58 V whereas upon the addition of Ni(II) ion there was not any change in oxidation peak, but two irreversible reduction peak at -1.33 V and -1.73 V appeared which correspond to

Ni(II)↔Ni(I) (Fig. 10). On the other hand S_2 showed remarkable change after the complexation with nickel ion. S_2 showed two oxidation peaks at 1.17 V, 0.96 V and two irreversible reduction peak at -0.44 V and -0.97 V. By the addition of Ni(II) ion one oxidation peak shifted positively as well as two irreversible peak shifted to -0.92 and -1.5 V which showed the complexation with nickel ion (Fig. 11) and Table 1. It is well observed that the redox potential of S_2 shift positively due to electron-withdrawing substituents. It may due to the electron withdrawing influence of the additional nitro group¹⁹.

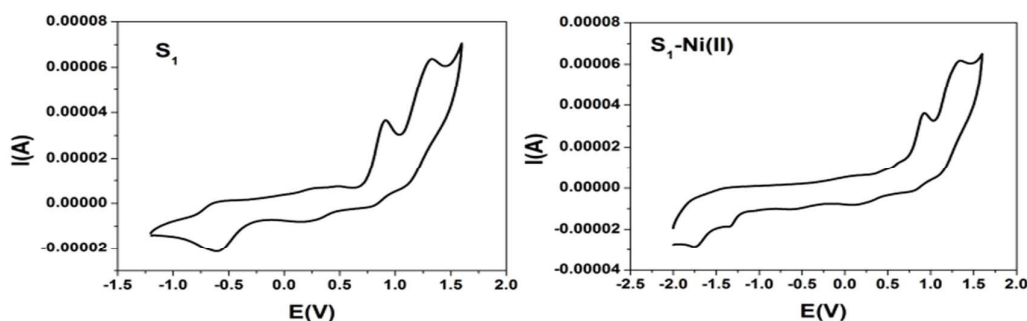


Fig.10 Cyclic voltammograms of S_1 and S_1 -Ni(II) complex in DMF solution containing 0.1 M TBAP at scan rate of 100 mVs^{-1} .

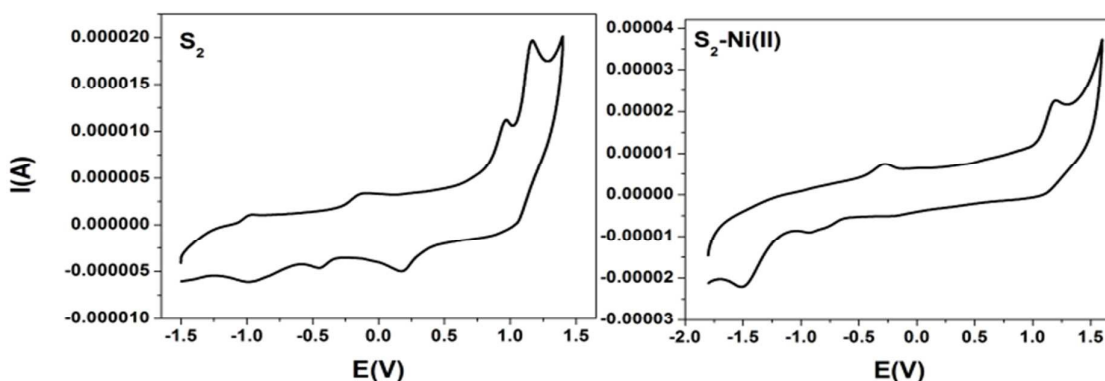


Fig. 11 Cyclic voltammograms of S_2 and S_2 -Ni(II) complex in DMF solution containing 0.1 M TBAP at scan rate of 100 mVs^{-1} .

Journal Name

ARTICLE

Table 1. The electrochemical behaviour of receptor S_1 , S_1 -Ni(II) and S_2 , S_2 -Ni(II) complexes.

Sample	I Oxid.(V)	II Oxid.(V)	I Red.(V)	II Red.(V)
Ligand S_1	0.91	1.33	-0.58	-
S_1 -Ni(II)	0.92	1.33	-1.33	-1.73
Ligand S_2	0.96	1.17	-0.44	-0.97
S_2 -Ni(II)	1.19	-	-0.92	-1.5

Theoretical calculation

In order to understand the mechanism of all obtained experimental results, a DFT study²⁰ was performed for molecular geometry and frequency calculation (ESI Fig. 8). The energy band gap between HOMO (3.79 eV), LUMO (2.74 eV) of S_1 and HOMO (3.39 eV), LUMO (2.50 eV) of S_2 has been decreased, i.e. 1.02 eV and 0.89 eV respectively (Fig. 13).

This represented a supportable mechanism for metal ion complexation according to the proposed coordination²¹. The HOMO→LUMO excitation was observed to favour the ligand to metal charge transfer (LMCT) which contributes to lowest energy excitation. It was notified that the energy decrease in LUMO level was remarkable than that in HOMO level, indicating that LUMO was more stabilized than HOMO. Attributed to the

importance of DFT studies, it was evaluated that apart from band gap the electron density in S_1 and S_2 was localized on the atoms of the whole molecule.

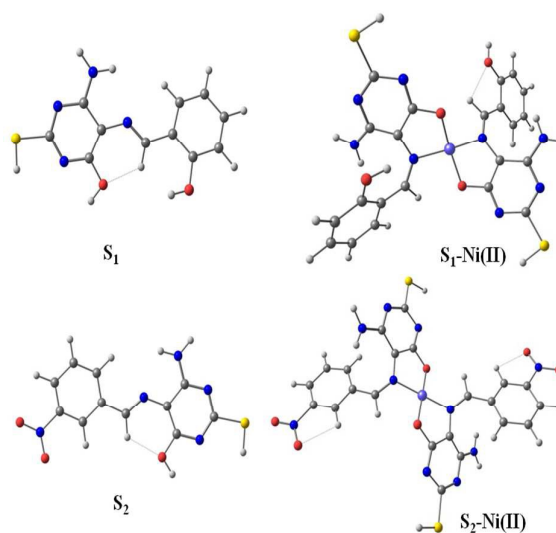


Fig.12 Optimized geometries of S_1 , S_1 -Ni(II) and S_2 , S_2 -Ni(II).

Upon the complexation with Ni(II) ion, the density was more located on S-Ni(II) complex. This result suggested that the coordination of Ni(II) with pyrimidine moiety promoted internal charge transfer through increasing the electron donating ability of the coordinating nitrogen and oxygen of pyrimidine moiety. Moreover the data of IR frequency of S_1 and S_2 had nearest spectrum to the experimental results (Fig. 12).

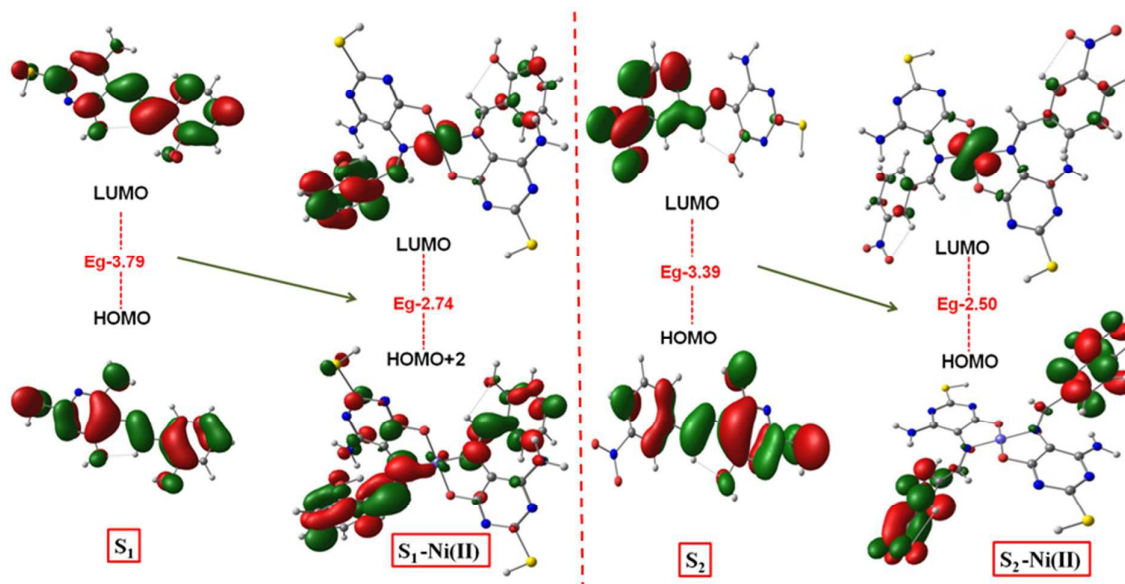


Fig. 13 Pictorial view of frontier molecular orbitals of S_1 , S_1 -Ni(II) and of S_2 , S_2 -Ni(II).

The reversibility behavior of S_1 and S_2

To explain the coordination mechanism of Ni(II) with receptors S_1 and S_2 , a fluorescence analysis has been done with EDTA. The reversibility test was performed using the S-Ni(II) solution ($5\mu\text{M}$) with disodium salt of ethylene diamine tetraacetic acid (EDTA) ($20\mu\text{M}$) in H_2O . The introduction of EDTA to S-Ni(II) solution could restore the yellowish color of receptors itself due to the strong binding ability of EDTA toward Ni(II). Both sensors were found to be reversible to its original state during the addition of EDTA and can be reused upto 3 cycles as demonstrated in Fig. 14. Both receptors have shown the quenching behavior with the addition of nickel

metal ion but as the EDTA added to the complex, the fluorescence intensity has been increased which clearly indicate that EDTA inhibit the interaction between receptor and metal ion²². Further addition of Ni(II) to the solution again quenching phenomena has been occurred. It is illustrated that the Ni(II) displayed a significant fluorescence change by showing the OFF behavior through complex formation. The addition of an excess amount of EDTA to the mixture of receptor S_1 -Ni(II) and S_2 -Ni(II) results in enhancing of the fluorescence intensity and hence acts as an ON switch (Fig. 14, 15). This “ON–OFF–ON” switching process could be repeated several times with the meager fluorescence efficiency loss.

The repeated behavior of S_1 , S_2 by fluorescence change with EDTA well explained the reversible behavior of both sensors which supports the electron transport mechanism for quenching.

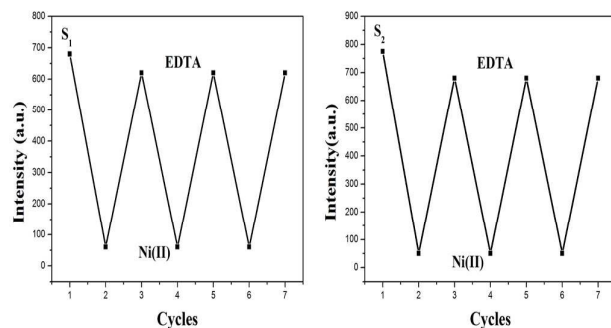


Fig. 14 Reversible changes in fluorescence intensity of S_1 , S_2 (5.0×10^{-6} M) at 520 nm, 441 nm respectively, after the sequential addition of Ni(II) and EDTA.

Logic gate application

Recent days, researchers have shown considerable interest towards molecular computing due to their broad application in molecular switches, keypad devices, biosensing, diagnostics, functional materials, biochemical systems²³ etc. As discussed above the reversibility behavior of both receptors, it can represent by the combinational logic circuit. In this concrete system (Fig. 15), the ON state (Output=1) is defined as the strong fluorescence at 520 nm (S_1) and 441 nm (S_2), whereas the OFF state (Output=0) corresponds to the weak fluorescence. The presence and absence of two chemical inputs IN1 Ni(II) and IN2 EDTA can be specified as '1' and '0' states. The threshold value of fluorescence intensity is stated 400 nm at output in case of both receptors. However, the enhanced

fluorescence of both receptors above the threshold level was ascertained in the absence (0, 0) and presence of both the inputs (1, 1) and also EDTA alone (1, 0). Therefore, observing the fluorescence of both receptors with the two-inputs (IN1 Ni(II) and IN2 EDTA), an IMPLICATION logic gate can be established at the molecular level (Fig. 15).

Analytical application

Analysis of nickel in waste and river water sample

Receptor S_1 was successfully applied for the determination of nickel metal ion in waste water samples²⁴. The water samples were collected from tap water of Roorkee, River Ganga from Roorkee and Haridwar. Absorption experiments were performed using 3 mL of S_1 (4×10^{-5} M in DMF) and 40 μ L of nickel metal ion (4×10^{-5} M) in corresponding water samples.

All water samples were used without a pretreatment, and known amount of nickel were added. The recovery of the receptor S_1 was obtained for different spiked water sample, calculated as 93.75-97.75% which was indicating that the application of receptor S_1 for the detection of Ni(II) in real water samples was quite doable. ESI Table 1 shows that the results analyzed by direct UV-Vis study are found to be close enough with calculated by atomic absorption spectroscopy (AAS) method with an appropriate amount of Ni(II) added and justify the potential of the optical sensor for routine measurements.

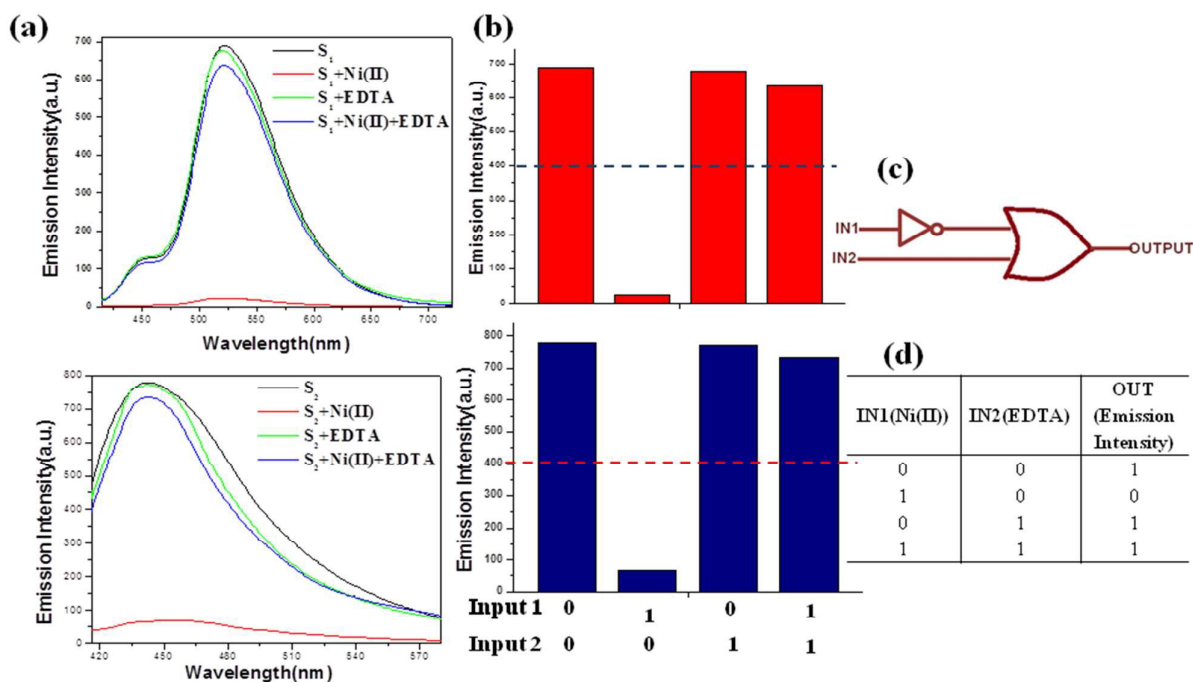


Fig. 15 (a) Fluorescence spectra of S₁ and S₂ (5 × 10⁻⁶ M) for an emission wavelength of 520 nm and 441 nm respectively under four different input conditions; (b) Changes in the fluorescence intensity at 520 nm (S₁) and 441 nm (S₂) under four different input conditions; (c) IMPLICATION logic scheme; (d) IMP truth table. IN1 and IN2 represent input Ni(II) ions and input EDTA, respectively; OUT are represented by their respective fluorescence intensity.

Conclusion

Here we have been synthesized two novel efficient colorimetric receptors via facile condensation process and characterized by various techniques. Upon addition of different metal ions, both receptors show a remarkable change in color (yellow to dark yellow) with Ni(II) metal ion which make suitable for easy naked eye detection. The 2:1 stoichiometry of S₁

and S₂ was confirmed by Job's plot, ESI Mass and ¹H NMR titration. The association constant values of S₁+Ni(II) and S₂+Ni(II) were calculated by Job's plot as 2.9 × 10⁶ and 2.1 × 10⁶ respectively. More interestingly, the fluorescence titration revealed that S₁ and S₂ behave as good fluorescence quencher, which support the electron transfer and nonradiative decay of excited state mechanism. The limit of detection

has been calculated as $33\mu\text{M}$ for $\text{S}_1+\text{Ni}(\text{II})$ and $48\mu\text{M}$ for $\text{S}_2+\text{Ni}(\text{II})$ that indicates S_1 is superior over S_2 . Electroanalytical studies have been investigated by the cyclic voltammetric experiment. Theoretical calculation suggests the complexation of both receptors with $\text{Ni}(\text{II})$ ion by the energy gap difference between HOMO and LUMO. Also, both receptors can work as a reversible sensor with EDTA on the basis of fluorescence titration. We are confident that both receptors are useful for practical application in other sensing fields such as biological and environmental research in the future.

Experimental details

Reagent

4,5-Diamino-6-hydroxy-2-mercaptopyrimidine, 3-nitro benzaldehyde and salicylaldehyde purchase from Sigma-Aldrich. All the salts of metals used were of analytical grade and used directly (without any further purification).

Instrumentation and Methods

The UV-Vis spectra were recorded on a Shimadzu, UV-3600 double beam spectrophotometer using 10 mm path length silica cell. FT-IR spectra were obtained with a Perkin Elmer FT-IR 1000 spectrophotometer as films between KBr. Elemental analysis were carried out on an Elementar model Vario EL-III. $^1\text{H-NMR}$ and $^{13}\text{C-NMR}$ spectra of S_1 and S_2 in DMSO-d_6 were recorded using Bruker AVANCE, 500.13 MHz spectrometer and Jeol ECX 400 MHz. Emission spectra were obtained

from RF-5301PC with a 3 cm standard quartz cell. LC-HRMS spectra were recorded on an Agilent spectrometer micrOTOF-Q II 10330 in positive mode using HPLC methanol as the solvent. Cyclic voltammetric studies were performed under nitrogen atmosphere at 298 K on a CHI760E electroanalyser in DMF with 0.1 M tetrabutylammonium perchlorate (TBAP) as supporting electrolyte. The working, reference and auxiliary electrodes were glassy carbon, Ag/AgCl and Pt wire, respectively, within the potential range $+1.5000\text{ V}$ to -1.5000 V at a scan rate of 0.1 V/s . All solution should be nitrogen purged before the experiment. Geometry optimization was performed using B3LYP functional with 6-31+g(d,p) basis sets as for receptors and with metal ion organize in the Gaussian 09 W programme in gas phase.

Synthesis and Characterization of S_1 and S_2

Synthesis of S_1

The proposed Schiff base S_1 was synthesized by stirring with reflux of 4,5-Diamino-6-hydroxy-2-mercaptopyrimidine (0.001M) with salicylaldehyde (0.001M) for 24 hours and after that a yellow color precipitate was observed.

Yield: (81%). IR data (KBr, $\nu_{\text{max}}/\text{cm}^{-1}$): O-H: 3434, N-H 3302, Ar-H: 3161, C=N: 1625, C=C: 1562, C-N: 1413, C-O: 1193. Anal.calc. for $\text{C}_{11}\text{H}_{10}\text{N}_4\text{O}_2\text{S}$: C, 50.37; H, 3.84; N, 21.36; O, 12.20 ; S, 12.23, Found: C, 49.98 ; H, 3.29 ; N,

20.89 ; O, 12.45 ; S, 12.14. UV-Visible (DMF, $\lambda_{\text{max}}/\text{nm}$) 392 nm ($n - \pi^*$), 290 nm ($\pi - \pi^*$), $^1\text{H-NMR}$ (DMSO- d_6 , 500 MHz, δ/ppm): 12.6 (s, 1H), 11.87 (s, 1H), 11.41 (s, 1H), 9.75 (s, 1H), 7.68 (d, 1H), 7.25 (d, 1H), 6.88 (m, 2H), 6.57 (s, 2H). $^{13}\text{C-NMR}$ (S_1 , DMSO- d_6 , 100 MHz, δ/ppm) 171, 158, 157, 155, 151, 136, 131, 130, 122, 119, 116. (ESI Fig.9 to 12).

Synthesis of S_2

To synthesize S_2 , took 0.01 M of 4,5-Diamino-6-hydroxy-2- mercaptopyrimidine and 0.01 M of 3-nitro benzaldehyde in methanol solution after that refluxed this solution with stirring for 10 hours till whole amount of amine was consumed, a yellow color precipitate was occurred.

Yield: (86%). IR data (KBr, $\nu_{\text{max}}/\text{cm}^{-1}$): O-H: 3452, N-H 3361, Ar-H: 3327, C=N: 1614, C=C: 1562, C-N: 1416, C-O: 1195. Anal.calc. for $\text{C}_{11}\text{H}_9\text{N}_5\text{O}_3\text{S}$: C, 45.36; H, 3.11; N, 24.04 ; O, 16.48; S, 11.01, Found: C, 44.83 ; H, 3.05 ; N, 24.89 ; O, 15.95 ; S, 11.14. UV-Visible (DMF, $\lambda_{\text{max}}/\text{nm}$) 374 nm ($n - \pi^*$) and 286 nm ($\pi - \pi^*$), $^1\text{H-NMR}$ Spectra: NMR (DMSO- d_6 , 500 MHz, δ/ppm): 12.06 (s, 1H), 11.92 (s, 1H), 9.76 (s, 1H), 8.65 (s, 1H), 8.33 (d, 1H), 8.18 (d, 1H), 7.68 (t, 1H), 6.98 (s, 2H). $^{13}\text{C-NMR}$ (S_2 , DMSO- d_6 , 100MHz, δ/ppm) 172, 157, 153, 149, 148, 140, 134, 130, 124, 121, 102 (ESI Fig.9 to 12).

Acknowledgement

NG is thankful to University of Grant Commission (UGC), New Delhi, India, for

financial support to undertake this work. NG is also grateful to Miss Pinky Yadav for her valuable discussion.

References

1. S. B. Mulrooney and R. P. Hausinger, *Microbiol. Rev.*, 2003, **27**, 239-261.
2. M. Bansal, D.Singh, V. K. Garg and P. Rose, *World Acad. Sci. Eng. Technol.*, 2009, **3**, 3-25.
3. G. Fu, Z. Hu, L. Xie, X. Jin, Y. Xie, Y. Wang, Z. Zhang, Y. Yang and H. Wu, *Int. J. Electrochem. Sci.*, 2009, **4**, 1052-1062.
4. M. Cempel and G. Nikel. *Polish J. of Environ. Stud.*, 2006, **3**, 375-382.
5. E. A. Takara, S. D. Pasini-Cabello, S. Cerutti, J. A. Gasquez and L. D. J. Martinez, *J. Pharm. Biomed. Anal.*, 2005, **39**, 735-739.
6. (a) M. Mazloum, M. S. Niassary and M. K. Amini, *Sens. Actuators, B*, 2002, **82**, 259-264. (b) M. Giorgetti, E. Scavetta, M. Berrettoni and D. Tonelli, *Analyst*, 2001, **126**, 2168-2171.
7. K. Jankowski, J. Yao, K. Kasiura, A. Jackowska and A. Sieradzka, *Spectrochim. Acta, Part B*, 2005, **60**, 369-375.
8. D. Zendelovska, G. Pavlovska, K. Cundeva and T. Stafilov, *Talanta*, 2001, **54**, 139-146.
9. A. Sunil, and S. J. Rao, *J. Anal. Chem.*, 2015, **70**, 154-158.
10. (a) S. Goswami , S. Chakraborty, S. Paul, S. Halder and A. C. Maity, *Tetrahedron Lett.*, 2013, **54**, 5075-5077. (b) D. Peralta-

- Domínguez, M. Rodríguez, G. Ramos-Ortiz, L. Maldonado, M. A. Meneses-Nava, O. Barbosa-García, R. Santillan, and N. Farfán, *Sens. Actuators, B*, 2015, **207** 511-517.
11. (a) L. Wang, D. Ye and D. Cao, *Spectrochim. Acta, Part A*, 2012, **90**, 40-44. (b) J. W. Nugent, H. Lee, H. Lee, J. H. Reibenspies, and R. D. Hancock, *Inorg. Chem.*, 2014, **53**, 9014–9026. (c) D. Singhal, N. Gupta and A. K. Singh, *Rsc. Adv.*, 2015, **5**, 65731-65738.
12. X. Liu, Q. Lin, T. Wei and Y. Zhang, *New J. Chem.*, 2014, **38**, 1418–1423.
13. (a) N. Gupta, A. K. Singh, S. Bhardwaj and D. Singhal, *Electroanalysis*, 2015, **27**, 1165-1175. (b) D. Singhal, A. K. Singh and A. Upadhyay, *Mater. Sci. Eng. C.*, 2014, **45**, 216-224.
14. T. Ghosh, B. G. Maiya and A. Samanta, *Dalton Trans.*, 2006, 795-801.
15. J. Liu, X. He, J. Zhang, T. He, L. Huang, J. Shen, Di Li, H. Qiu and S. Yin, *Sens. Actuators, B*, 2015, **208**, 538–545.
16. (a) H. Zhu, J. Fan, B. Wang and X. Peng, *Chem.Soc.Rev.*, 2014. (b) N. Aksuner, E. Henden, I. Yilmaz, and A. Cukurovali, *Sens. Actuators, B*, 2012, **166**, 269–274. (c) L. Fabbrizzi, M. Licchelli, P. Pallavicini, D. Sacchi and A. Taglietti, *Analyst*, 1996, **121**, 1763-1768. (d) Z. Li, W. Zhao, X. Li, Y. Zhu, C. Liu, L. Wang, M. Yu, L. Wei, M. Tang, and H. Zhang, *Inorg. Chem.*, 2012, **51**, 12444–12449. (e) M. Dutta and D. Das, *Trends Anal. Chem.*, 2012, **32**, 113-132.
17. (a) S. Sangeetha, G. Sathyaraj, D. Muthamilselvan, V. G. Vaidyanathan and B. U. Nair, *Dalton Trans.*, 2012, **41**, 5769-5773. (b) S. Blanchard, F. Neese, E. Bothe, E. Bill, T. Weyhermüller, and K. Wieghardt, *Inorg. Chem.*, 2005, **44**, 3636–3656. (c) Z. Li, W. Zhao, X. Li, Y. Zhu, C. Liu, L. Wang, M. Yu, L. Wei, M. Tang, and H. Zhang *Inorg. Chem.*, 2012, **51**, 12444–12449. (d) H. C. Clark, and R. J. O'Brien, *Can. J. Chem.*, 1961, **39**, 1030-1036.
18. A. Caballero, R. Martínez, V. Lloveras, I. Ratera, J. Vidal-Gancedo, K. Wurst, A. Ta'rraga, P. Molina, and J. Veciana, *J. Am. Chem. Soc.*, 2005, **127**, 15666-15667.
19. (a) K. Ghosh, V. Mohan, P. Kumar, S.W. Ng and E.R.T. Tiekink, *Inorg. Chim. Acta*, 2014, **416**, 76–84. (b) J. Jee, M. C. Chang, and C. Kwak, *Inorg. Chem. Commun.*, 2004, **7**, 614–617. (c) C. J. Dhanaraj and J. Johnson, *Spectrochim. Acta, Part A*, 2014, **118**, 624–631. (d) C. D. Pieve and B. Spingler, *Inorg. Chim. Acta*, 2012, **380**, 230–235. (e) A. Biswas, M. G. B. Drew and A. Ghosh, *Polyhedron*, 2010, **29**, 1029–1034. (f) B. Shafaatian, A. Soleymanpour, N. K. Oskouei, B. Notash and S. A. Rezvani, *Spectrochim. Acta, Part A*, 2014, **128**, 363–369.
20. H. B. Schlegel, G. E. Scuseria, M. A. Robb, J. R. Cheeseman, G. Scalmani, V. Barone, B. Mennucci, G. A. Petersson, H. Nakatsuji, M. Caricato, X. Li, H. P. Hratchian, A. F. Izmaylov, J. Bloino, G. Zheng, J. L. Sonnenberg, M. Hada, M. Ehara, K. Toyota,

- R. Fukuda, J. Hasegawa, M. Ishida, T. Nakajima, Y. Honda, O. Kitao, H. Nakai, T. Vreven, J. A. Montgomery, Jr., J. E. Peralta, F. Ogliaro, M. Bearpark, J. J. Heyd, E. Brothers, K. N. Kudin, V. N. Staroverov, R. Kobayashi, J. Normand, K. Raghavachari, A. Rendell, J. C. Burant, S. S. Iyengar, J. Tomasi, M. Cossi, N. Rega, J. M. Millam, M. Klene, J. E. Knox, J. B. Cross, V. Bakken, C. Adamo, J. Jaramillo, R. Gomperts, R. E. Stratmann, O. Yazyev, A. J. Austin, R. Cammi, C. Pomelli, J. W. Ochterski, R. L. Martin, K. Morokuma, V. G. Zakrzewski, G. A. Voth, P. Salvador, J. J. Dannenberg, S. Dapprich, A. D. Daniels, O. Farkas, J. B. Foresman, J. V. Ortiz, J. Cioslowski and D. J. Fox, Gaussian 09, Revision A.02, Gaussian, Inc., Wallingford CT, 2009.
21. B.B. Petkovi, M. Milci, D. Stankovi, I. Stamboli, D. Manojlovi, V.M. Jovanovi and S.P. Sovilj, *Electrochim. Acta*, 2013, **89**, 680–687.
22. Vesna D. Miletic, Auke Meetsma, Petra J. van Koningsbruggen and Zoran D. Matovic, *Inorg. Chim. Acta*, 2009, **12**, 720–723.
23. (a) Z. Dong, Y. Guo, X. Tian, and J. Ma, *J. Lumin.*, 2013, **134**, 635–639. (b) N. Kaur and P. Alreja, *Tetrahedron Lett.*, 2015, **56**, 182–186. (c) L. Huang, J. Zhang, X. Yu, Y. Ma, T. Huang, X. Shen, H. Qiu, X. He and S. Yin, *Spectrochim. Acta, Part A*, 2015, **145**, 25–32. (d) C. Zhang, C. Sun, Y. Lu, J. Wang, X. He, J. Lu, S. Yin and H. Qiu, *Spectrochim. Acta, Part A*, 2015, **150** 731–736.
24. M.R. Ganjali, M. Hosseini, M. Motalebi, M. Sedaghat, F. Mizani, F. Faridbod and P. Norouzi, *Spectrochim. Acta, Part A*, 2015, **140**, 283–287.

NJ-ART-08-2015-002118.R1

Table of Contents

Two simple and efficient energy transfer based fluorogenic receptors exhibiting high sensitivity for Ni^{2+} ion and its validation using DFT geometry optimization.

